Communications Medicine

https://doi.org/10.1038/s43856-026-01375-2

Article in Press

Metabolomic sweet spot clock predicts mortality and age-related diseases in the Canadian Longitudinal Study on Aging

Received: 4 November 2024

Accepted: 1 January 2026

Cite this article as: Vishnyakova, O., Min, J., Leach, S. *et al.* Metabolomic sweet spot clock predicts mortality and age-related diseases in the Canadian Longitudinal Study on Aging. *Commun Med* (2026). https://doi.org/10.1038/s43856-026-01375-2

Olga Vishnyakova, Joosung Min, Stephen Leach, Xiaowei Song, Kenneth Rockwood, Angela Brooks-Wilson & Lloyd T. Elliott

Metabolomic sweet spot clock predicts mortality and age-related diseases in the Canadian Longitudinal Study on Aging

Olga Vishnyakova[1,2,3,+], MSc, PhD, Joosung Min[3], MSc, Stephen Leach[1], BSc, Xiaowei Song[2,4], PhD, MSCS, Kenneth Rockwood[5], MD, Angela Brooks-Wilson[1,2,*], PhD, and Lloyd T. Elliott[3,*], PhD

[1] Department of Basic and Translational Research, BC Cancer, Vancouver, BC, Canada

[2] Department of Biomedical Physiology and Kinesiology, Simon Fraser University, Burnaby, BC, Canada

[3] Department of Statistics and Actuarial Science, Simon Fraser University, Burnaby, BC, Canada

[4] Surrey Memorial Hospital, Fraser Health, Surrey, BC, Canada

[5] Division of Geriatric Medicine, Dalhousie University, Halifax, NS, Canada, and Frailty & Elder Care Network, Nova Scotia Health, Halifax, NS, Canada

*These authors co-led the study.
+ ORCID: 0000-0002-7707-4740

Corresponding Author:

Lloyd T. Elliott, Department of Statistics & Actuarial Science, Simon Fraser University, Room SC K10545, 8888 University Drive, Burnaby, BC, Canada V5A 1S6, (778)782-3803, lloyd_elliott@sfu.ca

Alternate Corresponding Author:

abrooks-wilson@bcgsc.ca

Keywords: aging heterogeneity, CLSA, biomarker, metabolomics, healthy aging

Contributions

L.T.E. and A.B.W. developed and directed the project. O.V. developed and performed the modeling pipeline and wrote the original draft. S.L. processed and aliquoted study samples and curated data. J.M., X.S. and K.R. provided critical feedback on the study and reviewed/edited the manuscript. O.V. and L.T.E. prepared the manuscript with input from all authors and all authors approved the final manuscript.

Abstract

BACKGROUND

Chronological age does not capture individual health or resilience. Advances in metabolomics have enabled development of molecular aging biomarkers that capture deviations between biological and chronological age, highlighting how genetics, environment, and lifestyle shape biological aging. Despite their promise, metabolomic biomarkers face challenges such as interpretability, non-linearity, and reproducibility.

METHODS

We have developed a metabolomic predictor of biological age based on untargeted metabolomic profiling of individuals aged 45–85 years from the Canadian Longitudinal Study on Aging. To enhance interpretability, we first identified metabolites related to health based on variance heterogeneity. For metabolites with identifiable optimal levels, or "sweet spots", we modeled non-linearity using deviations from these values. A penalized regression model was trained on the Frailty Index using sweet spot deviations as predictors.

RESULTS

Here we show that the Sweet Spot Clock built on 178 health-related metabolites is strongly associated with all-cause mortality (HR=1.08, $p = 5.8 \times 10^{-12}$, C-index=0.841) and age-related diseases. The biomarker outperforms models trained on chronological age and those using raw metabolite levels, underscoring the importance of modeling non-linearity. It remains predictive after adjusting for age, sex, lifestyle and socioeconomic factors, though its added value over standard health and demographic measures is modest. The model generalizes to an independent cohort of individuals aged 85 years.

CONCLUSIONS

The Sweet Spot Clock provides a reproducible and interpretable measure of biological age. By modeling deviations from optimal metabolite levels and training on health status rather than age, it offers a tool for understanding aging heterogeneity and identifying individuals at risk of health decline.

Plain language summary

Chronological age does not fully reflect a person's health or resilience. We used data from Canadians aged 45–85 to develop a biomarker of biological age based on metabolites—small molecules in the blood that reflect body processes. We focused on 178 health-related metabolites and identified "sweet spots," or

optimal levels, for 74 of them. Our model, the Sweet Spot Clock, was strongly related to mortality and age-related diseases. These findings held up in an independent group of Canadians aged 85 and older. By focusing on health status and accounting for non-linear patterns, our approach offers a reproducible and interpretable way to measure biological aging and understand why some people age more healthfully than others.

Introduction

Aging is a universal process experienced uniquely by individuals. While chronological age is a strong proxy for biological age, it does not fully reflect individual variation in physiological and functional status. Biological age provides additional insight into health and the pace of aging among same-age individuals [1]. Although chronological age is a major risk factor for age-related diseases like type 2 diabetes, cardiovascular disease, and cancer [2], it does not consistently predict disease susceptibility, treatment response, or variability in aging trajectories. People of the same chronological age may show diverse aging phenotypes shaped by environmental exposures, lifestyle, psychological conditions, and genetic factors [3–5]. Discrepancies between chronological and biological age have led to a challenging search for reliable aging biomarkers—quantitative individual-level measures that predict biological age [6] and capture the variability in the timing of disease onset, functional decline, and mortality between individuals. Such biomarkers can act as predictors of aging, reflect the individual level of molecular and cellular damage, and provide valuable insights into what drives heterogeneity in aging.

To operationalize accurate aging biomarkers, numerous -omics clocks have been developed over the past decade [7–9], leveraging advancements in technology and longitudinal -omics data (e.g., epigenomics, metabolomics, proteomics, transcriptomics, immuneomics, glycomics, and the gut microbiome) [10–21]. These clocks typically target age deviation as a biomarker—the difference between predicted biological age and chronological age. Their weak inter-correlations indicate that they capture distinct facets of biological aging at various cellular levels, consistent with studies showing that metabolomic and epigenetic clocks often reflect complementary and non-overlapping biological processes [22]. Omics-based aging predictors are increasingly applied in research and clinical settings [6]. However, many models remain limited by the assumption of linearity [23,24], poor interpretability and high dimensionality, often relying on numerous predictors with unclear relevance to aging heterogeneity [25]. While non-linear methods such as neural networks are used to capture complex associations with aging outcomes, their black-box nature limits mechanistic insight [21]. There is a need for biomarkers that are interpretable, model non-linearity effectively, and are grounded in biologically relevant predictors. Metabolomics offers potential in this context, as metabolites reflect integrated signals from endogenous

processes and external exposures, including diet, lifestyle, and acute stress [26,27]. Though promising for identifying systemic markers of aging, challenges such as data reproducibility due to batch effects must be addressed [28].

In our previous work, we demonstrated that difference in variance between the least and the most healthy individuals at a given age can reveal phenotypes under homeostatic control, which we proposed to be closely related to health [29]. By narrowing the focus to metabolites potentially relevant to health, we can better target measurements that explain aging heterogeneity, reduce model complexity, minimize data noise, and enhance the interpretability of metabolomic clocks [6]. Moreover, our earlier findings showed that many phenotypes under homeostatic control demonstrate complex, non-linear associations with health, a pattern also noted in recent -omics studies [30]. Consequently, non-linear modeling or feature transformation techniques are necessary to address this complexity.

Here, we investigate the molecular bases of heterogeneity in aging by leveraging untargeted metabolomic profiling data from individuals in the Canadian Longitudinal Study on Aging [31]. We identify metabolites related to health and healthy aging and estimate their optimal levels, or "sweet spots." We construct a metabolomic aging biomarker that explicitly models deviations from these optimal values. The resulting Sweet Spot Clock is predictive of mortality and the onset of age-related diseases and provides a reproducible and interpretable measure of biological aging that replicates in an independent cohort of older adults.

Methods

Data

We examine data from the Canadian Longitudinal Study on Aging (CLSA) [31]. These data consist of a stratified sample of Canadian males and females aged 45 to 85 years. Community-dwelling participants were recruited by CLSA from the ten Canadian provinces excluding individuals unable to respond in English or French; residents of the three Canadian territories and some remote regions; individuals living on First Nation reserves and other First Nations settlements in the provinces or in nursing homes; full-time members of the armed forces; and individuals with significant cognitive impairment at recruitment. The subsample of participants selected for the Comprehensive Cohort (COM) of the CLSA underwent detailed physical assessments and provided blood and urine samples. Baseline data were collected between May 2012 and July 2015. The average follow-up period was six years, defined as the time between baseline and Follow-up 2 data collection. The onset of age-related diseases after baseline was determined using data from both Follow-up 1 and Follow-up 2 assessments.

Metabolomic profiling was done for 9,992 (51.5% females) out of 27,170 participants who provided blood samples at baseline. All participants of CLSA provided informed consent prior to data collection. The present study was approved by the joint Research Ethics Board of the BC Cancer and the University of British Columbia, and harmonized with Simon Fraser University (#H22-01012).

Genomic data

Genotyping was done by CLSA for 26,622 participants using the Affymetrix UK Biobank Axiom array, with phasing and imputation using TOPMed reference panel v.r2 [32]. CLSA performed marker-based and sample-based quality control [33]. Variants were examined for discordant genotype frequency between batches, departure from HWE, discordance across control replicates, and sex genotype frequency discordance. We removed low-quality imputed genetic variants: with a minor allele frequency lower than 0.1%, imputation quality score < 0.5, or missing rate > 0.1. The remaining 11.7 million variants were used for GWAS. Participants were examined for relatedness, sex discordance, outliers in heterozygosity and missing rates. Genetic ancestries were derived using principal component analysis and used to account for population structure. Sex was defined using genetically inferred sex chromosome composition as determined by CLSA [34]. Samples with discordance between genetically inferred sex and self-reported sex were excluded from analysis.

Untargeted metabolomic data and quality control

CLSA metabolomic data includes levels of 1,458 metabolites quantified in EDTA plasma samples by Metabolon using ultrahigh performance liquid chromatography–tandem mass spectroscopy (UPLC–MS/MS). A description of quality control and normalization is detailed elsewhere (https://www.clsa-elcv.ca/wp-content/uploads/2024/01/CLSA_DataSupportDoc_Metabolomics_v2.0_2023Aug03.pdf).

From an initial cohort of 9,992 participants with metabolomic data, we selected a maximal subset of unrelated individuals without third-degree or closer relatives [35]. We further excluded individuals that did not pass a sample-based quality control performed by CLSA. Specifically, we excluded samples with discrepancies between self-reported and genetic sex, as well as those exhibiting outlier values for missing genotype (>0.05%) data and heterozygosity rates (>0.215). The cohort used for analysis comprised 8,887 individuals with European ancestry, 111 individuals with Asian ancestry, and 63 individuals with Black ancestry, as previously categorized by CLSA. We omitted analytes with a missing data rate exceeding 20%, resulting in 1041 retained measures. Focusing on homeostatic mechanisms, the study was confined to endogenous metabolites, excluding xenobiotics, which were identified through annotations provided to

CLSA by Metabolon Inc. The final analytical dataset comprised 888 metabolites. Metabolite levels were log-transformed and scaled to ensure a mean of zero and standard deviation of one. To control for confounders, correlation analyses were performed between the metabolite levels and external factors, leading to adjustments in metabolite levels based on hours since the last meal or drink and dates of blood drawn. We applied an inverse rank-normal transformation to the metabolite ratios. Furthermore, we evaluated the metabolites for bimodality by ranking them using the bimodality index, where a bimodality index (BI) greater than 1.1 indicates potential bimodality, potentially affecting the reliability of the results [36]. The metabolites used for analysis and their bimodality indices are listed in Supplementary Data 1.

Replication cohort

Data from the Super Seniors Study was used as an independent replication cohort [37]. This study was approved by the joint Research Ethics Board of BC Cancer and the University of British Columbia, harmonized with Simon Fraser University (#H20-03117-A002). All participants gave written informed consent. Participants were determined to be Super Seniors if they met both of the following inclusion criteria: i) 85 years or older at the date of recruitment, and ii) self-reporting as never having had cancer (except non-melanoma skin cancer), cardiovascular disease, diabetes, dementia, or major pulmonary disease (except asthma). Controls were age-matched individuals who did not meet inclusion criteria. Non-fasting blood samples were collected from all participants. The data set comprised 548 Super Seniors and 119 age-matched controls. Self-reported sex was confirmed with genetically inferred sex chromosome composition, and genetic ancestry was inferred using principal component analysis.

EDTA plasma samples were sent to Metabolon for untargeted metabolomic profiling using Ultrahigh Performance Liquid Chromatography-Tandem Mass Spectroscopy (UPLC-MS/MS), yielding a total of 1,679 biochemicals, including 1,371 compounds of known identity. Raw data was extracted, peak-identified and processed using Metabolon's hardware and software. Peaks were quantified using area-under-the-curve. For each metabolite, the raw values in the experimental samples were divided by the median of those samples in each instrument batch, giving each batch and thus the metabolite a median of one. These data were also normalized to the QC samples for each batch similar to CLSA (https://www.clsa-elcv.ca/wp-content/uploads/2024/01/CLSA_DataSupportDoc_Metabolomics_v2.0_2023Aug03.pdf). Consistent with CLSA preprocessing, we performed minimum value imputation in which the minimum value detected for a given metabolite is used to replace the missing values for that same metabolite, followed by natural-log transformation and autoscaling

Instruments for health assessment

We derived five composite instruments to quantify health status, each standardized to a unit interval where higher scores reflect greater health burden. The first instrument (I) is a deficit accumulation Frailty Index (FI), calculated as the proportion of 51 health deficits present. The second (II) captures the frequency of five major diseases—cancer (excluding non-melanoma skin cancer), cardiovascular disease, chronic pulmonary disease, dementia, and diabetes—normalized by individual-level burden. The third (III) reflects the count of chronic conditions not included in the major disease category. The fourth (IV) assesses cognitive function using the average of three domain-specific scores, each rank-normalized from CLSA cognitive tests. The fifth(V) evaluates physical function based on rank-normalized scores from five physical performance assessments. Details on phenotype definitions and scoring procedures are provided in Supplementary Table 1. The construction and methodologies used for these instruments are described elsewhere [29]. We assigned health levels according to quartiles: healthiest, good health, fair health, and least healthy. Quartile-based cut-offs were applied to categorize participants by health levels regardless of age (Supplementary Table 2).

Statistics and Reproducibility

The study workflow is summarized in Fig. 1a,b and detailed in Supplementary Fig. 1. Primary analyses focused on the largest ancestral subset (European ancestry), representing 98% of the cohort. To perform inference and evaluate the performance of the molecular biomarkers, we randomly partitioned the participants with European ancestry into a training set (85%) and a validation (15%) set, resulting in sample sizes of 7,579 and 1,308, respectively. Sample sizes by sex and age group for the training and test sets are shown in Supplementary Table 3. The training set was used to subset metabolites, identify their optimal levels and to develop a model for estimating metabolomic age deviation. We stratified our analysis by sex, rather than adjusting for it, due to the substantial differences in metabolite concentrations and metabolic pathways observed between sexes [38]. Health scores and metabolite levels were adjusted for age.

Identifying health-related metabolites

We selected metabolites that exhibited a variance effect on health, meaning that variance among the healthiest group is significantly lower than among least healthy individuals. To perform this selection, we conducted pairwise tests of equality of variance between the metabolite levels of the healthiest and least healthy groups using the Brown-Forsythe (BF) test for heteroskedasticity [39].

Let $x \in \Re^N$ be metabolite level across N sample, p be a number of health groups, and $z_{ij} = \left|x_{ij} - \tilde{x}_j\right|$, where $\tilde{x}_j$ is the median of group j. The BF test statistic is the model F statistic:

$$F = \frac{(N-p)}{(p-1)} \frac{\sum_{j=1}^{p} n_j \left(\tilde{z}_{\cdot j} - \tilde{z}_{\cdot\cdot}\right)^2}{\sum_{j=1}^{p} \sum_{i=1}^{n_j} \left(z_{ij} - \tilde{z}_{\cdot j}\right)^2}$$

where n_j is the number of observations in group j, $\tilde{z}_{\cdot j}$ are the group means of the z_{ij} , and $\tilde{z}_{\cdot\cdot}$ is the overall mean of the z_{ij}. This F-statistic follows the F-distribution $\mathcal{F}_{p-1,\,N-p}$.

Analysis was stratified by sex. Metabolites were determined to be related to health and healthy aging if 1) the healthiest and least healthy groups had significantly different variance for at least one sex; and 2) the healthiest group had the lower variance. Bonferroni adjustment was used to account for multiple testing (Bonferroni correction factor N = 5 instruments x 2 sexes x 888 metabolites = 8880).

Defining metabolite optimal levels

We employed piecewise regression analysis (also known as segmented regression) to identify breakpoints indicating shifts in the impact on health deficit scores [40]. We defined the breakpoint as a single free parameter for which a continuous metabolite level modulates the mean response of a health deficit score through two linear segments joined at this breakpoint. For metabolite values X and the response health score Y, the piecewise regression equation for the expected mean $\mathbb{E}(Y|x,w) = \mu$ can be formulated as $\mu_i = w_i^T\gamma + \beta(x_i - \psi)1(x_i > \psi)$, where $i = 1,2,..n, \psi \in \mathcal{R}_X$ is a breakpoint, $1(\cdot) = 1$ when its argument is true, and $w_i^T\gamma$ includes additional linear terms, such as the model intercept, and possibly other covariates. The null hypothesis is $H_0: \beta = 0$, where β is the difference in slopes. The test statistic is a score-based statistics that follows the Normal distribution [41].

We identified optimal values, i.e., breakpoints under conditions where: 1) the slopes of the linear segments exhibit opposite signs; 2) the 95% confidence intervals for both slopes exclude zero; and 3) the disparity in slope values is statistically significant, as confirmed by a two-sided score test [42]. We assumed that the breakpoints remained constant across age group but varied by sex. To minimize age-related confounding, we adjusted health deficit scores for age prior to analysis and used the residual values for the piecewise regression. We conducted separate analyses for male and female sex to derive sex-specific estimates of the breakpoints. We used Bonferroni correction on the p-values of the piecewise regression to account for multiple comparisons (N= 5 instruments x 2 sexes x M metabolites), and deemed adjusted p-values below 0.05 to be statistically significant.

Distances from sweet spots

For each individual, the Euclidean distance (distances from sweet spots) was computed between the measured metabolite levels fitted to the piecewise regression model, and the optimal metabolomic levels. This method quantifies the deviation of actual metabolite concentrations from their optimal levels and reflects homeostatic dysregulation.

Developing metabolomic clocks

Following the idea that biomarkers of aging have to reflect not only inter-individual differences in mortality risk, but also the onset of age-related disease, we trained a penalized regression model to predict health status. We trained the sex-specific ElasticNet models to predict FI, serving as a surrogate endpoint for mortality, using health-related metabolites as predictors. For measurements for which we were able to estimate optimal levels, distances from sweet spots (DSSs) were used as transformation of metabolite levels. We refer to this model as the Sweet Spot Clock (Fig. 1c). To benchmark our approach against FI and established metabolomic clocks, we constructed comparator models that reflect key elements of prior frameworks trained on age [17] or untransformed metabolite levels [19], though these models were developed on targeted NMR platforms and focused on age or mortality rather than health decline. Specifically, we trained following four ElasticNet models:

1. SweetSpotClock. Health-related metabolites with DSS transformed levels were used as predictors. The model was trained to predict FI.

2. Baseline. This model reflects an established approach to contstructing -omic clocks. Health-related metabolites were used as predictors, with metabolite levels transformed into distances from their estimated optimal values. The model was trained to predict chronological age.

3. ControlAge: health-related metabolites with DSS transformed levels were used as predictors. The model was trained to predict chronological age. The model was trained to show the effect of training on FI, instead of chronological age, on predictive ability of all-cause mortality.

4. ControlMb: health-related metabolites without transformation levels were used as predictors. The model was trained to predict FI. The model was trained to show the effect of DSS transformation on predictive ability of all-cause mortality.

We applied 10-fold cross-validation to optimize the ElasticNet parameters on the training dataset. Post-training, we calibrated each model output to age units by rescaling predictions to match the mean and standard deviation of chronological age. We refer to these model outputs as metabolomic age. We then calculated metabolomic age deviation (MAD) for each participant by regressing biological age

against chronological age and taking the residual. The resulting age predictors (MADs) were then compared based on their association with mortality on the test set. ElasticNet feature importance was determined using *caret* R package [43].

Metabolic pathway enrichment analysis

We conducted pathway enrichment analysis to identify subpathways that were significantly enriched among the health-related metabolites. First, the significance ratio was calculated for each subpathway as the proportion of significant metabolites within the subpathway to the total number of measurements in that subpathway. The Fisher exact test was then used to determine significant enrichment [44], with Benjamini-Hochberg correction for multiple comparisons, controlling the false discovery rate at a significance level of 0.05.

Survival Analysis

We assessed associations between a biomarker and all-cause mortality using Cox proportional hazards models. All models were adjusted for sex and chronological age to account for potential confounders. Given the evidence that hazard ratio (HR) estimates are influenced by the scale and distribution of mortality predictors [45], we did not perform direct comparisons of HR estimates. Instead, we relied on Wald's test p-values for a scale-independent evaluation of the models and the concordance index (C-index). The predictive ability of biomarkers was assessed based on the performance on the test set.

Heritability estimate

To determine what portion of biomarker variability might be explained by the genetic component, we performed a GWAS on MAD. We used SAIGE [46] to obtain single-variant summary statistics, adjusting linear regressions for age, sex, and the first ten genetic principal components. We used LDSC (v1.0.1) [47] to estimate SNP-based heritability of MAD in CLSA COM using the LD scores from the 1,000 Genomes Project phase 3. We did not include the X chromosome in the LDSC computation, due to difficulties in assessing linkage disequilibrium in the X chromosome.

Association analysis

In CLSA, nutritional assessment was performed by the AB SCREEN II [48] and physical activity level was assessed by The Physical Activity Scale for Elderly [49]. Psychological distress was measured using Kessler Psychological Distress Scale[50]. Other factors were defined as follows: alcohol consumption (never, light/moderate, heavy drinker), household income (CDN <$20,000, $20,000–$50,000, $50,000–

<$100,000, $100,000–$150,000, >$150,000), education level (< secondary, secondary, post-secondary diploma/certification, or university degree), smoking status (never, occasional, current smoker, current heavy smoker). For more details on the CLSA protocol, see the CLSA Cohort profile. [31]

Comparison to established epigenetic clocks

Epigenetic age was assessed using two first-generation epigenetic clocks: the Hannum clock (based on 71 CpG sites [15]), and the Horvath Pan-Tissue clock (based on 353 CpG sites [14]). These biomarkers targeted chronological age during training process to estimate biological age. Both of these epigenetic clocks are included in the CLSA COM dataset. We also calculated PhenoAge and GrimAge using the Biolearn Python library [51]. While epigenetic data were available for 1,307 CLSA COM samples, only 161 were included in the validation set. To increase accuracy, we used the full dataset (both test and training sets) to estimate the strength of correlation between the Sweet Spot Clock and the epigenetic clocks. This approach was feasible because epigenetic data were not utilized in the training process.

Results

Health assessment and participants characteristics

To identify health-related metabolites, we first assessed the health status of all participants. A total of 9,061 individuals aged 45–86 years (51% females) from the CLSA Comprehensive cohort (CLSA COM) were included in the analysis of 1,458 plasma metabolites. Samples were collected by CLSA during the period from May, 2012 to July, 2015, with a mean tracking period of 6 years. The participants' mean body mass index was 28.1 (95% CI: 22.6-33.6) kg/m^2 and their mean fasting time before blood draw was 10 (95% CI: 6.5-13.5) hours. Out of a total of 9,061 individuals, 8,887 were of European ancestry, 111 of Asian ancestry, and 63 of Black ancestry. We conducted a primary analysis on the ancestry that was most numerous in the sample (European) and replicated our findings within the ancestries that were less numerous (Asian, Black).

To assign health scores to each participant, we developed five health instruments to measure health decline in older adults, as detailed in the Methods section: I - the Frailty Index (FI); II - the presence of five major diseases: cancer, cardiovascular disease, major pulmonary disease, dementia, and diabetes; III - the count of other chronic conditions; IV - a composite cognitive score; and V - physical function. All of these scores ranged from 0 (healthiest) to 1 (least healthy). The statistics and correlations between health scores are described in Supplementary Fig. 2.

Twenty percent of metabolites were identified as related to health

A total of 888 metabolites (60% of a total of 1,458 plasma metabolites) were examined for their relevance to health after excluding xenobiotics and those with more than 20% missing values (Supplementary Data 1). Among these, 686 metabolites (77%) with known identities were categorized into eight superpathways: lipid, amino acid, nucleotide, cofactor and vitamins, carbohydrate, peptide, partially characterized molecules, and energy.

We hypothesize that variance is lower in the healthiest group, for metabolites related to health. Therefore, we tested each metabolite for variance heterogeneity between the most and the least healthy groups. Samples were assigned to these two groups based on health scores quantiles (Methods). Of 888 metabolites tested, 178 (20%) showed statistically significant differences in variance at least for one health instrument and sex after Bonferroni correction for 8,880 tests (Supplementary Data 2); 137 of them had known identity. These measurements were selected as predictors of metabolomic age.

Among the 178 metabolites with detected sweet spots, 77 measurements (43%) were significant across male and female sexes (Fig. 2a). Metabolites involved in pentose, glycine, serine and threonine, and sterol metabolism showed differences in variance only in males. In contrast, metabolites from the pregnenolone and TCA Cycle pathways showed a variance effect on health exclusively in females. Analysis by superpathway revealed that amino acid, carbohydrate, and lipid superpathways harbored the most significantly heteroscedastic metabolites. The top markers that showed the strongest variance differences in these three superpathways were N6,N6,N6-trimethyllysine ($p=1.2x10^{-27}$), glucose ($p=1.2x10^{-20}$), and 1-stearoyl-2-linoleoyl-GPI (18:0/18:2) ($p=1.1x10^{-11}$), respectively (Supplementary Data 3).

We tested metabolites for their relevance to five different health instruments. Out of the 178 selected measurements, 137 (80%) showed significant variance differences between the most and least frail older adults. In contrast, only 7 metabolites showed variance heterogeneity between the groups highest and lowest in cognitive function, e.g. 1,5-anhydroglucitol (1,5-AG) ($p = 0.009$). Detailed information on metabolites related to each instrument and those shared between instruments is presented in Fig. 2b.

Only the androgenic steroids subpathway exhibited a statistically significant enrichment for health-related metabolites, with FDR adjusted p-value $6.8x10^{-7}$ (n=91). Other subpathways with notable significance ratios, calculated as a proportion of significant metabolites within the subpathway to the total number of measurements in that subpathway (see Methods), included ascorbate and aldarate metabolism, and corticosteroids. The top significant pathways determined by significance ratio are shown in Fig. 2c.

Most sweet spots estimates differ from population means

We identified optimal metabolite levels as breakpoints, where values above or below these thresholds were linked to poorer health. Using piecewise regression (see Methods), we determined optimal levels for 74 (42%) of the 178 selected metabolites (Supplementary Data 4) after Bonferroni-adjustment for 1,780 tests. Among these 74 measurements, we detected optimal level for 47 metabolites in older females, with the most significant effect change for gulonate (breakpoint estimate = -0.02, slopes = [-0.01, 0.04], $p=1.7x10^{-34}$). In older males, we were able to estimate optimal levels for 59 metabolites; the most significant effect change was for N6,N6,N6-trimethyllysine (breakpoint estimate = -0.31, slopes = [-0.11, 0.01], $p=1.7x10^{-34}$).

The different health instruments provided varying estimates for the breakpoint positions. However, overlap of the 95% confidence intervals suggests a common range of estimates among the instruments. We selected the breakpoint estimate with the narrowest 95% confidence interval (CI) as the optimal metabolite value, i.e. sweet spot (Fig. 3). Similar to the variance analysis, a piecewise regression on the Frailty Index (I) produced a sweet spot estimate for 59 out of 74 measurements (80%), compared to only 9 out of 74 measurements (12%) for cognitive function. The 95% CIs of the optimal values overlapped between sexes for only 12 metabolites (20%), including metabolonic lactone sulfate and gulonate. Further analysis revealed that for 41 metabolites (55%), the 95% CI for the optimal value did not include zero, which is CLSA population mean.

For each metabolite's sweet spot, we calculated the distance between the optimal level and the observed metabolite measurement for each individual. We also investigated the correlation between distances from metabolite sweet spots and chronological age along with health instruments (Supplementary Fig. 3). Among measurements with known identity, hydroxyasparagine** (Pearson $r^2=0.48$, $p=1.6x10^{-212}$) and dehydroepiandrosterone sulfate (DHEA-S) (Pearson $r^2=0.38$, $p=5.7x10^{-160}$), showed the strongest correlation between age and deviation from the metabolite's sweet spot.

Sweet spot distance transformation enhances the mortality association of the metabolomic aging biomarker

To estimate participants' metabolomic age, we trained the Sweet Spot Clock with a penalized regression model on the training set, using 178 identified health-related metabolites as predictors. For a subset of these, we used distances from estimated optimal values instead of the raw levels (Methods). The relationship between chronological age and predicted metabolomic age, the model prediction transformed into years, is illustrated in Fig. 4a. To be consistent with other -omics based biomarkers, metabolomic age

was regressed onto age to calculate metabolomic age deviation (MAD). The wide distribution of MAD (Fig. 4b) suggests substantial inter-individual variation and a rightward shift among women relative to men. We evaluated the performance of the proposed biomarker on the test set by comparing it to a null, a baseline, and control models based on discrimination accuracy, measured by the concordance index (C-index), and the strength of the association with 6-year all-cause mortality, both derived from Cox proportional hazards models.

The Sweet Spot Clock, trained on FI using distances from metabolite sweet spots, showed the strongest association with all-cause mortality and the highest discrimination (Wald statistic=6.9, $p = 5.8 \times 10^{-12}$, C-index=0.841). The baseline model (*Baseline* row in Table 2), an established metabolomic clock [17], showed lower discrimination (C-index=0.821) and a weaker association with all-cause mortality (Wald statistic=4.7, $p = 2.2 \times 10^{-6}$); this model was trained to predict chronological age from measured metabolite levels. The null model, with only age and sex as predictors, showed the lowest discrimination (C-index=0.809). Next, we investigated the contribution of two factors that resulted in improved performance compared to the baseline model: (1) training on FI instead of age and (2) transforming predictors by using distances from sweet spots instead of raw metabolite levels. To disentangle the contributions of each factor, we trained two additional models, each with one factor fixed: ControlAge (fixed target) and ControlMb (fixed predictors). Our results indicate that both targeting FI (Wald statistic=6.7, $p = 2.7 \times 10^{-11}$, C-index=0.839) and using distances from sweet spots (Wald statistic=5.0, $p = 4.5 \times 10^{-7}$, C-index=0.830) contributed to the overall improvement (Table 1). The correlations between metabolomic age derived from each model and the training targets (FI and age) are shown in Supplementary Fig. 4.

To complement the survival analyses, we also trained logistic regression models using 6-year mortality status (alive vs. dead) as a binary outcome. The ordering of biomarkers based on area under the curve (AUC) and accuracy was consistent with the C-index rankings from Cox models (Table 1). We additionally compared AUCs between models using the DeLong test; although the Sweet Spot model had the highest AUC, the pairwise differences were not statistically significant (Supplementary Table 4).

Metabolomic age deviation is strongly associated with mortality and onset of age-related diseases

Next, we evaluated prognostic ability of the metabolomic biomarker. We tested for the association with the onset of age-related conditions: diabetes, chronic obstructive pulmonary disease (COPD), stroke, kidney disease, Alzheimer's disease, and cancer. Besides mortality, MAD was associated with an increased risk of diabetes (HR = 1.05, $p = 8.9 \times 10^{-14}$, C-index=0.654), COPD (HR = 1.05, p =

$3.1x10^{-7}$, C-index=0.692), stroke (HR = 1.07, p = $2.1x10^{-4}$, C-index=0.712), and kidney disease (HR = 1.05, p = 0.02, C-index=0.641) after Bonferroni correction for 7 tests (Fig. 4d). All models showed higher discrimination accuracy than corresponding null models (with only sex and age as covariates; Table 2).

To examine the extent to which MAD associates with mortality, independently of age, we divided participants into age deviation groups based on their MAD quartile. We then performed survival analysis and found that the group with a higher level of the MAD biomarker in a test set had a 79% higher risk of mortality over the 6-year period compared to the group with a lower age deviation (HR=1.79; p = $8.7x10^{-6}$, C-index=0.821). The 6-year survival proportions by MAD quartiles are shown in Fig 4c. A complementary analysis using the 10th and 90th percentiles of MAD revealed an even stronger survival contrast (HR = 9.8; p = 6.5×10^{-5}, C-index = 0.85) between health extremes (Supplementary Fig. 5).

To improve robustness of our findings, we trained extended models, adjusting for additional covariates: body mass index (BMI), alcohol consumption, smoking status, physical activity level, and level of education (Methods). MAD remained strongly associated with mortality, diabetes, COPD, and stroke. Similarly, all models showed higher discrimination accuracy than corresponding extended null models (Table 2).

Metabolomic age deviation is strongly associated with lifestyle factors

Next, we explored genetic and environmental components of MAD. We conducted a genome-wide association study (GWAS) on MAD, which identified a single genomic region significantly associated with the aging biomarker at the genome-wide significance level. The region is located on chromosome 1 (1p36.32), with a leading intergenic SNP, rs11809159, downstream of the *AJAP1* gene (Fig. 4e). To assess the contribution of genetic factors to variability in MAD, we estimated SNP-based heritability using Linkage Disequilibrium Score Regression (LDSC). We found the SNP-heritability of MAD to be 0.23 (SE = 0.01). To investigate whether MAD and the Frailty Index shares common genetic component, we also performed a GWAS on the Frailty Index; however, all associations were below the genome-wide significance threshold.

We conducted an association analysis using univariate regression models on the test set to explore the relationship between MAD and health, lifestyle, and socioeconomic factors. Adjusted for sex and age, higher MAD was significantly associated with inflammatory biomarkers: High sensitivity C-reactive protein (β=0.02, p=$4.7x10^{-14}$), Tumor necrosis factor-alpha (β=0.04, p=$3.5x10^{-34}$), and Interleukin-6 (β=0.04, p=$2.2x10^{-32}$). MAD was also positively associated with psychological distress (β=0.08, p=$1.9x10^{-6}$), BMI (β=0.04, p=$2.2x10^{-32}$), Hemoglobin A1c, hyperglycemia biomarkers (β=0.04,

$p=2.5x10^{-39}$). Socioeconomic variables revealed that lower household income ($\beta=-0.03$, $p=8.1x10^{-17}$) and educational attainment ($\beta=-0.01$, $p=2x10^{-3}$ were associated with higher MAD. Lifestyle factors—nutrition quality ($\beta=-0.2$, $p=1.5x10^{-22}$), smoking ($\beta=0.02$, $p=1.7x10^{-11}$), and alcohol consumption ($\beta=0.03$, $p=4.7x10^{-5}$), also demonstrated strong associations with elevated MAD. To test for association between MAD and chronic condition load (number of conditions determined by Instrument II and Instrument III), cognitive (Instrument IV) and physical (Instrument V) function, we additionally adjusted regression models for BMI, alcohol consumption, smoking, education and physical activity level resulting in strong associations. All p-values were Bonferroni-adjusted for n=15 tests (Table 3).

Metabolomic biomarker and mortality-predictive epigenetic biomarker share signals of aging heterogeneity

To understand the relationship with other -omics-based biomarkers, we measured the correlation between MAD and epigenetic age deviation as measured by five established epigenetic clocks. We observed weak correlations with the Hannum clock [15] ($r^2 = 0.12$, $p = 2.0x10^{-4}$), the Horvath Pan-Tissue clock [14] ($r^2 = 0.08$, $p = 0.005$) and DNAm PhenoAge[13] ($r^2 = 0.17$, $p = 3.3x10^{-7}$). In contrast, the correlation with DNAm GrimAge [45] adjusted for chronological age appeared to be moderate ($r^2 = 0.38$, $p = 2.3x10^{-44}$ for GrimAge v1). For additional details on correlations between the omics clocks (constructed metabolomic clocks and established epigenetic clocks) in both the full dataset and the test set, see Supplementary Fig. 6 and Supplementary Fig. 7, respectively.

To further explore the predictive performance of the proposed metabolomic biomarker, we conducted a secondary analysis in a subset of 1,242 individuals (64 mortality events) with paired metabolomic and DNA methylation data. In this subgroup, the Sweet Spot Clock demonstrated higher discrimination than established epigenetic clocks (C-index: 0.783 for Sweet Spot Clock vs. 0.751 for GrimAge v2). A combined multi-omics model incorporating both MAD and GrimAge v2 achieved the highest discrimination (C-index = 0.806; Supplementary Table 5).

Metabolite-level insights into biological age deviation

Next, we examined the metabolites' contribution to the calculated age deviation. In total, the Frailty Index-based model for predicting MAD resulted in 126 unique predictors, 100 of which have known identity. Of these 126 metabolites, 111 and 78 were retained in the female and male models, respectively, following separate Elastic Net selections (Supplementary Data 5). In the female model, hydroxyasparagine** ($\beta=0.0074$), mannose ($\beta=0.0049$), and erythronate* ($\beta=0.0047$) contributed the most to Frailty Index. For the male model, mannose ($\beta=0.0039$), (S)-3-hydroxybutyrylcarnitine ($\beta=0.0037$), and vanillactate ($\beta=0.0032$) were among the top contributors to MAD. As an additional

control, we tested the 50 top predictive metabolites for associations with 40 known disease biomarkers, chronic conditions, and diagnostic measurements, adjusting for age and sex. All analytes showed strong associations after Bonferroni correction (n=2000) with at least five distinct phenotypes tested (Supplementary Fig. 8).

Replication of associations of MAD with health status and mortality

To replicate association between MAD, health decline and mortality, we performed untargeted metabolomic profiling on 667 participants from the Super Seniors Study [37] using EDTA plasma samples. For each batch, the data were normalized to the same QC samples as were used by CLSA (Methods), which allowed us to apply the previously identified CLSA sweet spots to the Super Seniors data. We then computed MAD scores using the original, pretrained Sweet Spot Clock without retraining. The data set comprised 548 exceptionally healthy Super Seniors aged 85 and older (mean age = 89, SD = 3.5, 62% females) who have never been diagnosed with cancer, cardiovascular or pulmonary disease, diabetes or dementia; and 119 age-matched controls with one or more chronic diseases (mean age = 89, SD = 3.7, 52% females); 612 (92%) were of European ancestry.

First, we calculated MAD for each participant, resulting in a mean age deviation -0.4 years among the Super Seniors (SD=3.1) versus 1.1 years (SD=3.5) among controls. Logistic regression for the all-cause mortality target adjusted for age, sex and ancestry (European/non-European), resulted in significant association between MAD and Super-Senior/age-matched control phenotype (β=0.15, SE=0.03, OR=1.16, $p=2.8\times10^{-6}$, Supplementary Fig. 9). Next, we conducted survival analysis using 658 individuals with known status, 334 of whom died by the status date. After adjusting for age, sex and ancestry, MAD showed significant association with mortality (HR=1.08, SE=0.02, $p=3.3\times10^{-5}$, Supplementary Fig. 10), and higher discrimination (C-index=0.66) than the null model with only age, sex and ancestry as covariates (C-index=0.61).

To test generalizability, we calculated MAD for CLSA participants with Asian or Black ancestry, comprising 111 and 63 individuals with metabolomic data, respectively, who had not withdrawn from the CLSA by the second follow-up. There were no deaths among the subset with Asian ancestry and three deaths in the subset with Black ancestry. Cox regression, adjusted for sex and age, did not reveal a significant association between the MAD and all-cause mortality among the subset with Black ancestry (HR=1.15, SE=0.12, p=0.26).

Discussion

We have introduced the Sweet Spot Clock, a metabolomic predictor of biological age. Our model restricts to metabolites related to health, and demonstrates that deviations from optimal metabolite values are better predictors of biological age than metabolite levels alone. To the best of our knowledge, this is the first study to explicitly account for non-linearity in metabolomic data. Our blood-based biomarker was strongly associated with all-cause mortality and health-related outcomes. Replication in an independent, older cohort demonstrated the generalizability of the Sweet Spot Clock, although predictive performance was attenuated, likely reflecting age-related metabolic shifts and cohort differences. These findings are consistent with previous research on the metabolome, which has shown that an older predicted metabolomic age compared to chronological age is associated with multiple risk factors for premature mortality [25]. Our model also showed strong correlations with comorbidity burden, physical decline, and cognitive decline, while exhibiting weak correlation with epigenetic age deviation computed by the DNAm PhenoAge, Hannum, and Horvath Pan-Tissue clocks, and moderate correlation with the GrimAge clock that incorporates smoking status and clinical biomarkers. A preliminary multi-omics model combining MAD with GrimAge v2 achieved the highest predictive performance in the paired subset than any individual predictor along, highlighting a promising future direction. These results further confirm that metabolomic models effectively capture differences in biological age independent of epigenetic changes [25].

As expected, age and sex were the strongest predictors of age-related outcomes. While the extended model incorporating lifestyle and socioeconomic factors sometimes achieved higher concordance, the Sweet Spot Clock captured distinct biological variation not explained by these variables. For stroke and kidney disease, it even outperformed conventional predictors (i.e., BMI, alcohol consumption, smoking status, physical activity, and education) combined, suggesting added value in specific domains. These findings highlight the biomarker's potential to complement established predictors and offer mechanistic insight into why individuals age differently, even if its standalone clinical utility is modest.

To investigate why some individuals remain healthier and experience a later onset of age-related diseases compared to their peers, we focused on deficit accumulation across multiple systems, and trained a statistical model on the Frailty Index (an intermediary target) instead of on age or mortality. Many large-scale biobank studies have developed metabolomic clocks primarily trained to predict chronological age [52]. While these studies demonstrated strong associations with mortality risk, cardiovascular phenotypes, and various disease risk factors, our findings suggest that focusing on deficit accumulation results in superior performance in predicting mortality and age-related diseases. Generally speaking, models trained to accurately predict chronological age do not capture the underlying biological

variability. These models focus on aligning with the chronological timeline rather than identifying the physiological changes and risk factors associated with different health outcomes. Another study employed targeted plasma metabolomics to develop metabolomic risk scores trained on all-cause mortality [19]. Although mortality is a clearly defined endpoint and has been used in several recent studies, including GrimAge [45], training statistical models on functional decline or deficit accumulation has a clear advantage. Elucidating dysregulated pathways associated with health decline provides an opportunity for lifestyle or medical intervention. Although deficit accumulation reflects established physiological changes and a degree of resilience loss, it currently represents a comprehensive and clinically meaningful proxy for multisystem health decline in population-based studies. By training metabolomic models on this intermediary phenotype, our approach aims to extract biological signals that precede overt clinical manifestations. This framework offers a path toward refining instruments to capture earlier stages of dysregulation along the aging trajectory.

Previous multi-omics analysis of the Frailty Index reported metabolites and genetic variants associated with frailty in female twins [53]. While our GWAS analyses did not reveal any significant associations, we were able to replicate some metabolite-FI associations — glutamate, C-glycosyltryptophan, pseudouridine, and epiandrosterone sulfate were among the metabolomic predictors of FI. Additionally, C-glycosyltryptophan, erythronate, and androstenediol (3beta,17beta) disulfate (2) were previously associated with all-cause mortality in the Alpha-Tocopherol, Beta-Carotene Cancer Prevention Study Cohort [54].

As observed in previous work on Super Seniors [55] and validated in previous work on phenotypic measures, lower variance among the healthiest group is key to elucidating health-related measurements [29]. Instead of selecting measurements based on correlation with age, we concentrated on the effect on health to explain differences in aging processes. Variance analysis resulted in a number of metabolic predictors, many of which were already related to diseases. For instance, N6,N6,N6-trimethyllysine (TML) and glucose demonstrated significant variance effects on health, serving as key indicators of disruptions in metabolic pathways such as carnitine synthesis and epigenetic variation [56] and glucose metabolism. Previous studies have shown an association between elevated TML and glucose levels with metabolic disorders, including diabetes and cardiovascular diseases [57–59]. Aconitate has been suggested as a diagnostic marker for mitochondrial aconitase deficiency resulting in mitochondrial dysfunction [60]. Levels of analytes with unknown identity also varied with health, suggesting the presence of significant yet uncharacterized metabolites that may provide additional understanding of metabolic functions and disorders. Overall, by defining health-related metabolites through the lens of variance, we were able to

gain meaningful insights into homeostatic regulation and prioritize the most significant analytes for further analysis.

Relationship analysis revealed metabolites that were not previously known to have sweet spots. Notably, we sought to identify age-independent optimal metabolite levels. While previous studies indicate that age significantly influences metabolomic profiles [61,62], it is likely that that the observed variability may be attributed more to differential maintenance of metabolic health rather than to the aging process itself. Notably, the majority of the estimated optimal levels deviated from the population mean, suggesting that older adults, on average, are not in optimal health. Although average population values are often used to assess dysregulation levels of individuals, they may not accurately represent health [63].

Higher TML levels were previously associated with elevated risk of all-cause and cardiovascular mortality [58]. Our findings extend this observation by showing that levels below the optimal range are also associated with worse health. Increased metabolonic lactone sulfate levels were previously associated with cardiometabolic disease in a Mexican American population-based cohort [64], while low levels had not been associated with adverse outcomes, but our analyses imply that deviations in either direction from an optimal value are relevant to health.

This study has several limitations. Firstly, 98% of the CLSA study population analyzed consisted of individuals of European ancestry, limiting the generalizability of the findings to diverse ancestries. To address the limited generalizability, it is crucial for future research to include diverse populations. The metabolome is inherently noisy and influenced by factors such as diet and environmental exposures [25], making longitudinal metabolomic data necessary, though correction for batch effects remains challenging [28]. Untargeted metabolomic profiling with relative concentrations of metabolites prevented us from calculating specific optimal levels. Although this study offers strong support for relative locations of sweet spots, further analysis is needed to establish optimal metabolite levels in absolute concentrations, for potential clinical use. Comparisons between our biomarker and established epigenetic clocks should be interpreted with caution. The epigenetic clocks were trained on external datasets that differ from CLSA in age structure, phenotypic breadth, mortality follow-up, and population characteristics. Finally, while we included comparator models reflecting the design principles of age-based (i.e., MetaboAge[17]) and mortality-based models (i.e., MetaboHealth[19]), direct benchmarking against these established clocks is limited by platform differences (targeted NMR vs. untargeted LC-MS) and distinct training endpoints. Our approach therefore complements rather than replicates existing metabolomic clocks, emphasizing health-related decline and non-linear transformations.

To summarize, our study identified metabolites related to health and estimated their optimal levels. We developed a sweet spot metabolomic clock that predicts biological age and examined the genetic and environmental components of age deviation. Associations between the metabolomic biomarker, health decline, and mortality were replicated in an independent cohort of individuals aged 85 years and older.

Data availability

Data are available from the Canadian Longitudinal Study on Aging (www.clsa-elcv.ca) for researchers who meet the criteria for access to de-identified CLSA data. The Super Seniors dataset is stored at Genome Sciences Center, BC Cancer, Canada. For inquiries about this dataset, or for requests to collaborate on projects involving this dataset, please contact Dr. Angela Brooks-Wilson at abrooks-wilson@bcgsc.ca. The list of metabolites used for analysis is provided in Supplementary Data 1. Source data for recreating figures are available at https://zenodo.org/records/17594106 [65] and in Supplementary Data Files 2-7: The source data for Fig. 2 a, b is in Supplementary Data 2, the source data for Fig. 2 c is in Supplementary Data 3, the source data for Fig. 3 is in Supplementary Data 4, the source data for Fig. 4 d is in Supplementary Data 6, and the source data for Fig. 4 e is in Supplementary Data 7. The list of predictors included in the Sweet Spot Clock model is in Supplementary Data 5.

Disclaimer. The opinions expressed in this manuscript are the authors' own and do not reflect the views of the Canadian Longitudinal Study on Aging.

Conflict of Interest

The authors declare that they have no conflict of interest.

Code availability

All code used in this study is available at https://zenodo.org/records/17594106 [65] The data analysis was performed in R v. 4.4.2.

ACKNOWLEDGMENTS

This research is funded by the Canadian Institutes of Health Research (grant # PAD 179760) to A Brooks-Wilson and LT Elliott. LT Elliott's research is supported by a Michael Smith Health Research BC Scholar Award. This research was made possible using the data collected by the Canadian Longitudinal Study on Aging (CLSA). Funding for the Canadian Longitudinal Study on Aging (CLSA) is provided by the Government of Canada through the Canadian Institutes of Health Research (CIHR) under grant

reference: LSA 94473 and the Canada Foundation for Innovation, as well as the following provinces, Newfoundland, Nova Scotia, Quebec, Ontario, Manitoba, Alberta, and British Columbia. This research has been conducted using the CLSA Baseline Comprehensive Dataset version 7.0, Follow-up 1 Comprehensive version 4.0, Follow-up 2 Comprehensive version 1.0, Genomic data version 3.0, Epigenetics version 1.1, Metabolomics version 2.0 under Application Number 2206033. The CLSA is led by Drs. Parminder Raina, Christina Wolfson and Susan Kirkland. The AB SCREEN™ II assessment tool is owned by Dr. Heather Keller. Use of the AB SCREEN™ II assessment tool was made under license from the University of Guelph.

REFERENCES

1. Lowsky, D. J., Olshansky, S. J., Bhattacharya, J. & Goldman, D. P. Heterogeneity in healthy aging. *J Gerontol A Biol Sci Med Sci* 69, 640–649 (2014).
2. Rae, M. J. *et al.* The demographic and biomedical case for late-life interventions in aging. *Sci Transl Med* 2, (2010).
3. van den Berg, N. *et al.* Longevity defined as top 10% survivors and beyond is transmitted as a quantitative genetic trait. *Nat Commun* 10, (2019).
4. Chiu, M. *et al.* Mortality risk associated with psychological distress and major depression: A population-based cohort study. *J Affect Disord* 234, 117–123 (2018).
5. Stringhini, S. *et al.* Socioeconomic status, non-communicable disease risk factors, and walking speed in older adults: multi-cohort population based study. *BMJ* 360, (2018).
6. Moqri, M. *et al.* Biomarkers of aging for the identification and evaluation of longevity interventions. *Cell* 186, 3758–3775 (2023).
7. Lohman, T., Bains, G., Berk, L. & Lohman, E. Predictors of Biological Age: The Implications for Wellness and Aging Research. *Gerontol Geriatr Med* 7, (2021).
8. Jylhävä, J., Pedersen, N. L. & Hägg, S. Biological Age Predictors. *EBioMedicine* 21, 29–36 (2017).
9. Rutledge, J., Oh, H. & Wyss-Coray, T. Measuring biological age using omics data. *Nat Rev Genet* 23, 715–727 (2022).
10. Lehallier, B. *et al.* Undulating changes in human plasma proteome profiles across the lifespan. *Nat Med* 25, 1843–1850 (2019).
11. Peters, M. J. *et al.* The transcriptional landscape of age in human peripheral blood. *Nat Commun* 6, (2015).
12. Tanaka, T. *et al.* Plasma proteomic signature of age in healthy humans. *Aging Cell* 17, (2018).
13. Levine, M. E. *et al.* An epigenetic biomarker of aging for lifespan and healthspan. *Aging* 10, 573–591 (2018).
14. Horvath, S. DNA methylation age of human tissues and cell types. *Genome Biol* 14, (2013).
15. Hannum, G. *et al.* Genome-wide methylation profiles reveal quantitative views of human aging rates. *Mol Cell* 49, 359–367 (2013).
16. Menni, C. *et al.* Metabolomic markers reveal novel pathways of ageing and early development in human populations. *Int J Epidemiol* 42, 1111 (2013).
17. Van Den Akker, E. B. *et al.* Metabolic age based on the BBMRI-NL 1H-NMR metabolomics repository as biomarker of age-related disease. *Circ Genom Precis Med* 13, 541–547 (2020).

18. Robinson, O. *et al.* Determinants of accelerated metabolomic and epigenetic aging in a UK cohort. *Aging Cell* 19, (2020).
19. Deelen, J. *et al.* A metabolic profile of all-cause mortality risk identified in an observational study of 44,168 individuals. *Nat Commun* 10, (2019).
20. Galkin, F. *et al.* Human Gut Microbiome Aging Clock Based on Taxonomic Profiling and Deep Learning. *iScience* 23, (2020).
21. Sayed, N. *et al.* An inflammatory aging clock (iAge) based on deep learning tracks multimorbidity, immunosenescence, frailty and cardiovascular aging. *Nat Aging* 1, 598–615 (2021).
22. Kuiper, L. M. *et al.* Epigenetic and Metabolomic Biomarkers for Biological Age: A Comparative Analysis of Mortality and Frailty Risk. *J Gerontol A Biol Sci Med Sci* 78, 1753–1762 (2023).
23. Okada, D., Cheng, J. H., Zheng, C., Kumaki, T. & Yamada, R. Data-driven identification and classification of nonlinear aging patterns reveals the landscape of associations between DNA methylation and aging. *Hum Genomics* 17, (2023).
24. Tanaka, T. *et al.* Plasma proteomic biomarker signature of age predicts health and life span. *Elife* 9, 1–24 (2020).
25. Robinson, O. & Lau, C. H. E. Measuring biological age using metabolomics. *Aging* 12, 22352–22353 (2020).
26. Rattray, N. J. W. *et al.* Metabolic dysregulation in vitamin E and carnitine shuttle energy mechanisms associate with human frailty. *Nat Commun* 10, 11 (2019).
27. Adav, S. S. & Wang, Y. Metabolomics Signatures of Aging: Recent Advances. *Aging Dis* 12, 646–661 (2021).
28. Yu, Y. *et al.* Correcting batch effects in large-scale multiomics studies using a reference-material-based ratio method. *Genome Biol* 24, 1–26 (2023).
29. Vishnyakova, O., Song, X., Rockwood, K., Elliott, L. T. & Brooks-Wilson, A. Physiological phenotypes have optimal values relevant to healthy aging: sweet spots deduced from the Canadian Longitudinal Study on Aging. *Geroscience* 46, 1589–1605 (2024).
30. Shen, X. *et al.* Nonlinear dynamics of multi-omics profiles during human aging. *Nat Aging* https://doi.org/10.1038/S43587-024-00692-2 (2024) doi:10.1038/S43587-024-00692-2.
31. Raina, P. *et al.* Erratum: Cohort Profile: The Canadian Longitudinal Study on Aging (CLSA)(International Journal of Epidemiology (2019) 2019 DOI: 10.1093/ije/dyz173). *Int J Epidemiol* 48, 2066 (2019).
32. Taliun, D. *et al.* Sequencing of 53,831 diverse genomes from the NHLBI TOPMed Program. *Nature 2021 590:7845* 590, 290–299 (2021).
33. Forgetta, V. *et al.* Cohort profile: genomic data for 26 622 individuals from the Canadian Longitudinal Study on Aging (CLSA). *BMJ Open* 12, (2022).
34. Forgetta, V. *et al.* The Canadian Longitudinal Study on Aging Genome-wide Genetic Data Release (version 3). https://www.cog-genomics.org/plink/1.9/formats.
35. Bycroft, C. *et al.* The UK Biobank resource with deep phenotyping and genomic data. *Nature* 562, 203–209 (2018).
36. Wang, J., Wen, S., Fraser Symmans, W., Pusztai, L. & Coombes, K. R. The bimodality index: a criterion for discovering and ranking bimodal signatures from cancer gene expression profiling data. *Cancer Inform* 7, 199–216 (2009).

37. Halaschek-Wiener, J. *et al.* The Super-Seniors Study: Phenotypic characterization of a healthy 85+ population. *PLoS One* 13, (2018).
38. Darst, B. F., Koscik, R. L., Hogan, K. J., Johnson, S. C. & Engelman, C. D. Longitudinal plasma metabolomics of aging and sex. *Aging* 11, 1262–1282 (2019).
39. Brown, M. B. & Forsythe, A. B. Robust tests for the equality of variances. *J Am Stat Assoc* 69, 364–367 (1974).
40. Muggeo, V. M. R. Estimating regression models with unknown break-points. *Stat Med* 22, 3055–3071 (2003).
41. Muggeo, V. M. R. Testing with a nuisance parameter present only under the alternative: a score-based approach with application to segmented modelling. *J Stat Comput Simul* 86, 3059–3067 (2016).
42. Muggeo, V. M. R. Interval estimation for the breakpoint in segmented regression: a smoothed score-based approach. *Aust N Z J Stat* 59, 311–322 (2017).
43. Kuhn, M. Building Predictive Models in R Using the caret Package. *J Stat Softw* 28, 1–26 (2008).
44. Rivals, I., Personnaz, L., Taing, L. & Potier, M. C. Enrichment or depletion of a GO category within a class of genes: which test? *Bioinformatics* 23, 401–407 (2007).
45. Lu, A. T. *et al.* DNA methylation GrimAge strongly predicts lifespan and healthspan. *Aging* 11, 303–327 (2019).
46. Zhou, W. *et al.* Efficiently controlling for case-control imbalance and sample relatedness in large-scale genetic association studies. *Nat Genet* 50, 1335–1341 (2018).
47. Finucane, H. K. *et al.* Partitioning heritability by functional annotation using genome-wide association summary statistics. *Nat Genet* 47, 1228–1235 (2015).
48. Keller, H. H., Goy, R. & Kane, S. L. Validity and reliability of SCREEN II (Seniors in the Community: Risk evaluation for eating and nutrition, Version II). *European Journal of Clinical Nutrition 2005 59:10* 59, 1149–1157 (2005).
49. Washburn, R. A., McAuley, E., Katula, J., Mihalko, S. L. & Boileau, R. A. The Physical Activity Scale for the Elderly (PASE): Evidence for Validity. *J Clin Epidemiol* 52, 643–651 (1999).
50. Kessler, R. C. *et al.* Screening for serious mental illness in the general population. *Arch Gen Psychiatry* 60, 184–189 (2003).
51. Ying, K. *et al.* A Unified Framework for Systematic Curation and Evaluation of Aging Biomarkers. *bioRxiv* 2023.12.02.569722 (2024) doi:10.1101/2023.12.02.569722.
52. Moqri, M. *et al.* Validation of biomarkers of aging. *Nat Med* 30, 360–372 (2024).
53. Livshits, G. *et al.* Multi-OMICS analyses of frailty and chronic widespread musculoskeletal pain suggest involvement of shared neurological pathways. *Pain* 159, 2565–2572 (2018).
54. Huang, J. *et al.* Serum Metabolomic Profiling of All-Cause Mortality: A Prospective Analysis in the Alpha-Tocopherol, Beta-Carotene Cancer Prevention (ATBC) Study Cohort. *Am J Epidemiol* 187, 1721–1732 (2018).
55. Halaschek-Wiener, J. *et al.* Reduced telomere length variation in healthy oldest old. *Mech Ageing Dev* 129, 638–641 (2008).
56. Maas, M. N., Hintzen, J. C. J., Porzberg, M. R. B. & Mecinović, J. Trimethyllysine: From Carnitine Biosynthesis to Epigenetics. *Int J Mol Sci* 21, 1–33 (2020).
57. Vekic, J., Silva-Nunes, J. & Rizzo, M. Glucose Metabolism Disorders: Challenges and Opportunities for Diagnosis and Treatment. *Metabolites* 12, (2022).

58. Bjornestad, E. O. *et al.* Trimethyllysine predicts all-cause and cardiovascular mortality in community-dwelling adults and patients with coronary heart disease. *European heart journal open* 1, (2021).
59. Li, X. S. *et al.* Untargeted metabolomics identifies trimethyllysine, a TMAO-producing nutrient precursor, as a predictor of incident cardiovascular disease risk. *JCI Insight* 3, (2018).
60. Abela, L. *et al.* Plasma metabolomics reveals a diagnostic metabolic fingerprint for mitochondrial aconitase (ACO2) deficiency. *PLoS One* 12, (2017).
61. Trabado, S. *et al.* The human plasma-metabolome: Reference values in 800 French healthy volunteers; impact of cholesterol, gender and age. *PLoS One* 12, (2017).
62. Johnson, L. C. *et al.* Amino acid and lipid associated plasma metabolomic patterns are related to healthspan indicators with ageing. *Clin Sci (Lond)* 132, 1765–1777 (2018).
63. Cohen, A. A. *et al.* Statistical distance as a measure of physiological dysregulation is largely robust to variation in its biomarker composition. *PLoS One* 10, (2015).
64. Das, S. K. *et al.* Metabolomic architecture of obesity implicates metabolonic lactone sulfate in cardiometabolic disease. *Mol Metab* 54, (2021).
65. Vishnyakova, O. *et al.* Data for: Metabolomic sweet spot clock predicts mortality and age-related diseases in the Canadian Longitudinal Study on Aging. Zenodo. https://doi.org/10.5281/ZENODO.17594106

TABLES

Table 1. The associations between metabolomic age deviations (MAD) and all-cause mortality.

Model*	Target	DSS	C-Index	HR	95% CI	p-value**	AUC***	Accuracy
Sweet Spot Clock	**FI**	**+**	**0.841**	**1.08**	**[1.06-1.10]**	**5.8×10^{-12}**	**0.824**	**0.951**
ControlMb	FI	-	0.839	1.08	[1.06-1.11]	2.7×10^{-11}	0.822	0.950
ControlAge	Age	+	0.830	1.10	[1.06-1.14]	4.5×10^{-7}	0.824	0.950
Baseline	Age	-	0.821	1.09	[1.05-1.13]	2.2×10^{-6}	0.815	0.950
Frailty index	-	-	0.830	1.05	[1.02-1.07]	5.2×10^{-5}	0.809	0.948
Null	-	-	0.809	-	-	-	0.795	0.949

* Association were determined by Cox proportional hazards models, on the test (1285 participants who had not withdrawn from the study by the second follow-up with 69 death events). Each model has been adjusted for sex and age. MAD are the residuals of metabolomic clocks, calibrated into units of age, and then regressed onto age. Hazard ratios (HRs) of MAD corresponding to each model are shown alongside their 95% confidence intervals (CIs). The line corresponding to the proposed metabolomic predictor is highlighted in bold.

** The p-values were obtained from two-sided Wald's tests.

*** AUC and accuracy were estimated for logistic regressions on 6-year mortality status, adjusted for age and sex.

Table 2. The associations between metabolomic age deviations (MAD) and age-related diseases, as determined by Cox proportional hazards models.

Outcome	Model*	C-Index	HR	95% CI	p-value**
Mortality	MAD	0.841	1.08	[1.06-1.10]	$8.1x10^{-11}$
N=1285, N events=69	Null	0.809	-***	-	-
	MAD Extended	0.863	1.09	[1.06-1.13]	$2.2x10^{-7}$
	Null Extended	0.851	-	-	-
Diabetes	MAD	0.654	1.05	[1.04-1.07]	$1.8x10^{-13}$
N=942, N events=236	Null	0.594	-	-	-
	MAD Extended	0.676	1.04	[1.03-1.06]	$1.8x10^{-6}$
	Null Extended	0.656	-	-	-
COPD	MAD	0.692	1.05	[1.03-1.07]	$6.2x10^{-7}$
N=1063, N events=108	Null	0.655	-	-	-
	MAD Extended	0.757	1.05	[1.02-1.06]	0.001
	Null Extended	0.746	-	-	-
Stroke	MAD	0.712	1.07	[1.04-1.11]	$4.2x10^{-4}$
N=1108, N events=30	Null	0.649	-	-	-
	MAD Extended	0.723	1.07	[1.03-1.11]	0.02
	Null Extended	0.673	-	-	-
Kidney disease	MAD	0.641	1.05	[1.02-1.08]	0.04
N=1096, N events=49	Null	0.594	-	-	-
	MAD Extended	0.652	1.05	[1.01-1.08]	0.07
	Null Extended	0.618	-	-	-
Cancer	MAD	0.642	1.00	[0.98-1.02]	1
N=962, N events=194	Null	0.642	-	-	-
	MAD Extended	0.656	1.00	[0.98-1.02]	1
	Null Extended	0.655	-	-	-
Dementia or Alzheimer's	MAD	0.908	0.92	[0.80-1.06]	1
disease	Null	0.896	-	-	-
N=1126, N events=5	MAD_Extended	0.955	0.94	[0.79-1.11]	1
	Null_Extended	0.954	-	-	-

* Each model was adjusted for sex and age. Hazard ratios (HRs) of MAD corresponding to each model are shown alongside their 95% confidence intervals (CIs). MAD are the residuals of Sweet Spot Clock, calibrated into units of age, and then regressed onto age. Null model had age and sex as predictors. Extended models were additionally adjusted for body mass index, alcohol consumption, smoking status, physical activity level, and a level of education.

** The p-values were obtained from two-sided Wald's tests and Bonferroni adjusted (n=14).

*** HRs shown in this table correspond to the metabolomic biomarker only, as they quantify its added predictive value beyond the covariates. The Null and Extended Null models do not include the biomarker and therefore do not provide an HR. HRs for all covariates in all models are reported in Supplementary Data 6.

Table 3. The associations between metabolomic age deviations (MAD) and multiple factors on the test. Associations were evaluated using linear regression models adjusted for age and sex, with two-sided Wald tests of regression coefficients. P-values were Bonferroni-adjusted (n=17). MAD are the residuals of Sweet Spot Clock, calibrated into units of age, and then regressed onto age.

	Factor	beta	SD	p-value
Overall health	Chronic condition count	0.008	0.001	8.5×10^{-36}
	Physical function (Instrument IV)	0.003	0.001	2.8×10^{-9}
	Cognitive function (Instrument V)	0.002	0.001	5.6×10^{-5}
Body composition	Body Mass Index	0.037	0.003	2.2×10^{-32}
Inflammation	Interleukin-6	0.036	0.003	2.2×10^{-32}
	Tumor Necrosis Factor - Alpha	0.043	0.003	8.5×10^{-36}
	High Sensitivity C-Reactive Protein, mg/L	0.018	0.002	4.7×10^{-14}
Hyperglycemia	Hemoglobin A1c, %	0.041	0.003	2.3×10^{-39}
Lifestyle	Nutritional Risk	-0.203	0.019	1.5×10^{-22}
	Smoking status	0.017	0.002	1.7×10^{-11}
	Alcohol consumption	0.032	0.007	4.7×10^{-5}
	Physical activity levels	0.037	0.003	8.5×10^{-36}
	Psychological Distress	-1.200	0.225	1.8×10^{-6}
Socio-economic	Total household income	-0.030	0.003	8.1×10^{-17}
	Level of Education	-0.011	0.003	2.0×10^{-3}

FIGURE LEGENDS

Fig. 1. Overview of the approach (a) and analysis workflow (b). We assessed health status for each participant using five instruments and assigned health scores. Plasma metabolites from the baseline assessment were tested to identify those presumed to be related to health by examining variance heterogeneity between health groups. For measurements with established non-linear relationships with health deficits, metabolite levels were transformed by calculating the distances between measurements and optimal metabolite levels. These optimal levels, or "sweet spots," were estimated using piecewise regression on health deficit. Health-associated metabolites were then used to construct a predictive model for metabolomic age. The deviation between metabolomic and chronological age formed the molecular biomarker, metabolomic age deviation. Subsequent CLSA follow-up visits were used only to ascertain chronic condition status (Created with BioRender.com).

Fig. 2. Metabolites identified as health-related. **a**, Variance differences between the most and least healthy groups. The bars depict the -log10 of p-values from the two-sided Brown-Forsythe test, with only the lowest p-values across all health instruments and sexes displayed. Metabolite names are color-coded: black indicates significantly lower variance in the healthiest group across both sexes, green for males only, and orange for females only. **b**, Shared health-related metabolites across health instruments. Orange bars in the y-axis represent the total number of metabolites with significantly lower variance among healthiest group as determined by each health instruments. Black bars in the x-axis represent the number of metabolites shared across instruments. **c**, Metabolic subpathways enriched in health-related metabolites. P-values are from the two-sided Fisher's exact test, adjusted for multiple testing (n=91) using Benjamini-Hochberg correction. Instruments: I - the Frailty Index; II - the number of five diseases: cancer (except non-melanoma skin cancer), cardiovascular disease, major pulmonary disease, dementia, and diabetes; III - the number of other chronic conditions; IV - cognitive function; V- physical function. The source data for Fig. 2 is in Supplementary Data 2-3.

Fig. 3. Estimated optimal levels for health-related metabolites. The forest plot represents estimated optimal levels for 74 metabolites. Optimal levels and their 95% confidence intervals (CIs) were estimated using piecewise regression. The central point of each error bar corresponds to the regression-estimated optimal level, and the bars indicate its 95% CIs. The narrowest CI for each metabolite, across all health instruments, is displayed. The heatmap represent -log10(p-values) associated with the strength of the effect of metabolite levels on health, as determined by five instruments. P-values from the two-sided score test were Bonferroni-adjusted (n=1780). Instruments: I - the Frailty Index; II - the number of five diseases: cancer (except non-melanoma skin cancer), cardiovascular disease, major pulmonary disease,

dementia, and diabetes; III - the number of other chronic conditions; IV - cognitive function; V- physical function. The source data for Fig. 3 is in Supplementary Data 4.

Fig. 4. Metabolomic age deviation predicts mortality and age-related diseases. **a**, Chronological age versus metabolomic age. Each dot represents a CLSA COM participant, darker meaning >1 individual. R indicates Pearson correlation between variables; p-value is for a two-sided t-test. Values above the regression line (dashed black line) indicates faster agers; below the line - slower agers. **b**, Distribution of metabolomic age deviation (in years). **c**, 6-year survival proportions by metabolomic age deviation (MAD) quartiles. Cox proportional hazard model was adjusted for age and sex. P-value was estimated by two-sided Wald test. **d**, Hazard ratios for various adverse outcomes derived from Cox hazard regression models adjusted for sex and age (mortality, n=1,285; diabetes, n=942; COPD, n=1,063; stroke, n=1,108; kidney disease, n=1,096; cancer, n=962; dementia, n=1,126). The covariate in the model is metabolomic age deviation. The central point of each error bar corresponds to the estimated hazard ratio, with horizontal lines indicating the 95% confidence interval. P-values for two-sided Wald's tests are adjusted for seven tests using Bonferroni correction. **e**, Genome-wide association study of metabolomic age deviation (genomic control $\lambda = 1.049$). Association statistics were obtained from two-sided Wald tests. Grey horizontal line indicates genome-wide significance level of P < 5E-8. A single genomic region significantly associated with the aging biomarker at the genome-wide significance level (rs11809159, p-value=1.94×10^{-9}). The source data for Fig. 4 is in Supplementary Data 6-7.

Editorial summary:
Vishnyakova et al. develop a metabolomic aging biomarker based on optimal metabolite levels, or "sweet spots." They show that this biomarker predicts mortality and the onset of age-related diseases.

Peer review information: *Communications Medicine* thanks Sithara Vivek, Chiara Herzog and Valentin Vetter for their contribution to the peer review of this work.

a

Canadian Longitudinal Study on Aging

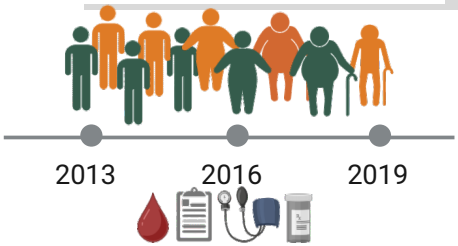

n = 9,061 Females: 51% Age: 45-86

Participant profile

Health assessment

- Frailty Index
- 5 major diseases count
- Chronic conditions count
- Physical function
- Cognitive function

Untargeted metabolomics

Genotype data

DNA methylation

Lifestyle

Aging heterogeneity analysis

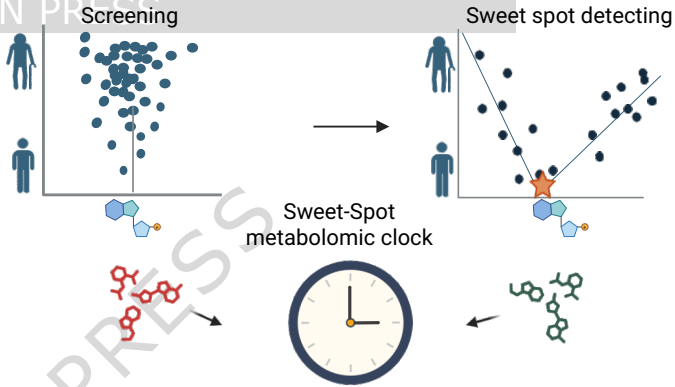

b

1. Assess participants' health
2. Identify metabolites related to health
3. Identify metabolites' sweet spots
4. Develop Sweet Spot Clock using distances from sweet spots
5. Test for association with mortality and onset of age-related diseases
6. Explore genetic and environmental components
7. Replication

c

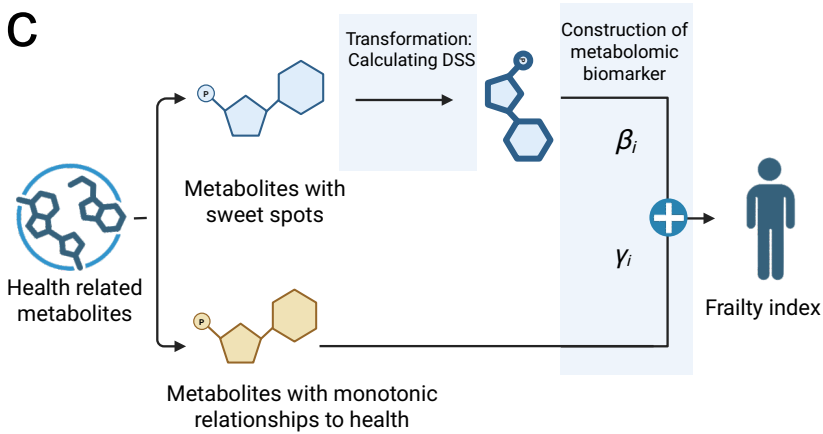

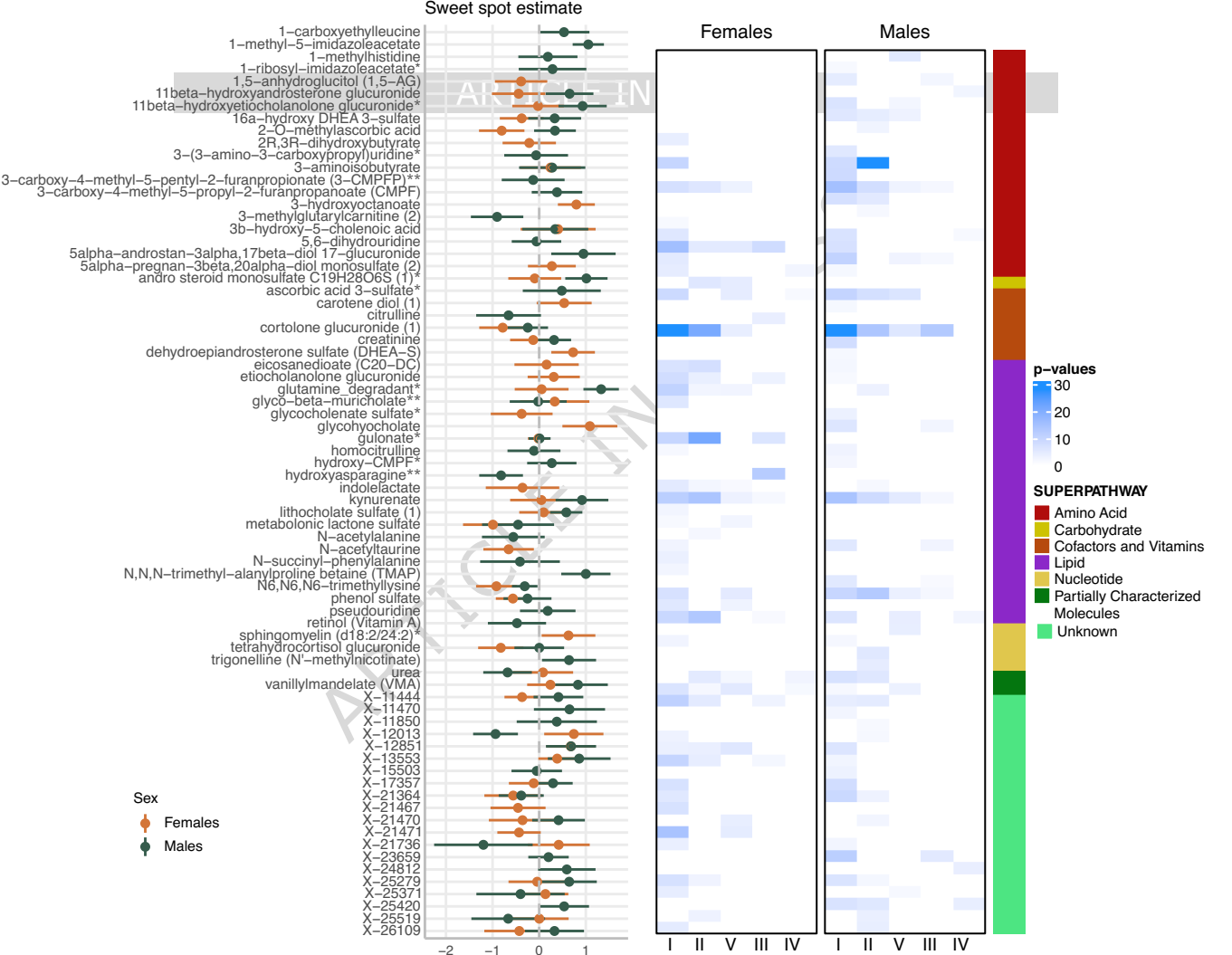

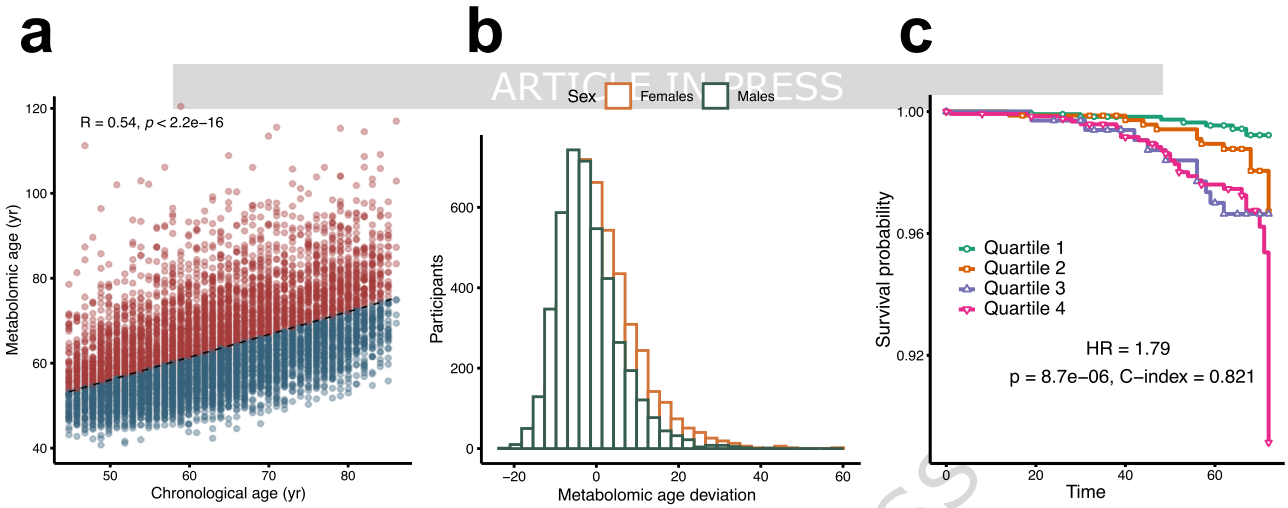

d

Outcome	Hazard Ratio (95% CI)	p−value
All−cause mortality	1.08 (1.06−1.10)	8.1e−11
Diabetes	1.05 (1.03−1.08)	1.8e−13
COPD	1.05 (1.03−1.09)	6.2e−07
Stroke	1.07 (1.01−1.10)	4.2e−04
Kidney failure	1.05 (1.00−1.09)	0.036
Alzheimer's	0.92 (0.73−1.03)	1.0
Cancer	1.00 (0.96−1.02)	1.0

e